Charith Abhayaratne · Deepayan Bhowmik

Scalable Watermark Extraction for Real-time Authentication of JPEG 2000 Images

Abstract This paper proposes a novel scalable authentication scheme that utilizes the progressive enhancement functionality in JPEG 2000 scalable image coding. The proposed method first models the wavelet-based quality scalable coding to identify the effect of the quantization and de-quantization on wavelet coefficient magnitudes and the data embedded within such coefficients as a watermark. A relationship is then established between the watermark extraction rule and the embedding rule, using the magnitudes of the reconstructed and original coefficients. It ranks the wavelet coefficients according to their ability to retain the embedded watermark data intact under various quantization levels corresponding to quality enhancements. Then watermark data is embedded into wavelet coefficients according to their rank followed by JPEG 2000 embedded coding. At the decoder as more and more quality and resolution layers are decoded the authentication metric is improved, thus resulting in gradually increasing complexity of the authentication process according to the number of quality and resolution enhancements. The low complexity authentication is available at low quality low resolution decoding, enabling real-time authentication for resource constrained applications without affecting the authentication metric. Compared to the existing methods, the proposed method results in highly robust scalable authentication of JPEG 2000 coded images.

Keywords

Scalable authentication, wavelet-based watermarking, JPEG 2000, quality scalability, watermark robustness.

1 Introduction

Image authentication based on watermarks involves embedding an unique logo or a fingerprint data into the host image and extracting them at the time of authentication. Influenced by its success in scalable image coding, the discrete wavelet transform (DWT) has been widely used in image watermarking [1–21]. Based on the embedding methodology, wavelet-based image watermarking can be categorized into two main classes: uncompressed domain algorithms [1–13] and joint compression-watermarking algorithms [14–21]. In the former, the authentication requires decoding the image to its pixel level to performing the forward DWT again to extract the watermark to carry out authentication. This two step process increases the complexity of the authentication and makes it difficult for real-time authentication. The second approach integrates watermarking into the compression process, mainly

Department of Electronic and Electrical Engineering, The University of Sheffield, Sheffield, S1 3JD, United Kingdom
E-mail: c.abhayaratne@sheffield.ac.uk
E-mail: d.bhowmik@sheffield.ac.uk

considering JPEG 2000 [22], by avoiding the repeating of the forward DWT. The watermark is embedded into quantized wavelet coefficients followed by embedded coding. Although their main aim is to improve the robustness of watermarking to JPEG 2000 compression, these algorithms do not utilize the quality and resolution scalability functionalities available in JPEG 2000. JPEG 2000 Part 8 (ISO/IEC 15444-8, T.807) Secure JPEG 2000 (JPSEC) [15] specifies a framework, concepts, and methodology for securing JPEG 2000 bit streams considering capabilities of JPEG 2000 and also proposes watermarking in the coding pipeline with aim of achieving high robustness as a solution [21, 23].

The scalability in bit streams produced by scalable coding enables progressive enhancement of quality and resolution of image and video content being displayed. Scalable image coding consists of multi-resolution decomposition of images (using the DWT), followed by hierarchical layered representation considering the scalability requirements: quality and resolution, mainly. In JPEG 2000, the hierarchical layered representation is based on the progressive coding of bit planes of wavelet coefficients and increasing wavelet decomposition scales. The most common application scenario is that the image is encoded to the highest quality and highest resolution generating a bit stream, followed by adapting the bit stream according to the available bandwidth before transmission. The quality and the resolution of the decoded image are enhanced when more and more bits are received from the scalable bit stream. If the watermark embedding algorithm does not consider the scalability of the host image bit stream, such content adaptations result in loss of watermark data embedded within the affected coefficients, thus, diminishing the robustness of the watermarking schemes [24].

In this paper, we propose a novel scalable authentication scheme that utilizes the progressive enhancement functionality in JPEG 2000. The proposed method first models the wavelet-based quality scalable coding to estimate the effect of the quantization and de-quantization on wavelet coefficient magnitudes and the data embedded within such coefficients as a watermark. A relationship is then established between the watermark extraction rule and the embedding rule, using the magnitudes of the reconstructed and original coefficients. This relationship ranks the wavelet coefficients according to their ability to retain the embedded watermark data intact under various quantization levels corresponding to quality enhancements. The watermark data is embedded into wavelet coefficients according to their rank, followed by embedded coding of coefficients in JPEG 2000. We propose different conditions considering the two extraction scenarios: blind and non-blind. Since the watermark data is embedded in wavelet coefficients chosen according to the hierarchy of quality resolution layers, as opposed to the coefficients chosen by raster scanning of wavelet subbands as in other methods, meaningful authentication data can be extracted even from the very low bit rate decoding. As more and more quality and resolution layers are decoded at the decoder, the authentication metric is improved, thus resulting in gradually increasing complexity of the authentication process with respect to the increasing quality and resolution enhancements. Due to its low complexity authentication at low quality low resolution decoding, the proposed algorithm enables real-time authentication for resource constrained applications without affecting the authentication metric.

The rest of the paper is organized as follows: Section 2 presents the background preliminaries for the proposed work. The model considering non-blind extraction for magnitude alteration-based watermark embedding is presented in Section 3, while the model considering blind extraction for re-quantization-based watermark embedding is presented in Section 4. The experimental verification of the proposed models are shown in Section 5. The performance evaluation of the proposed scalable authentication is presented in Section 6, followed by the concluding remarks in Section 7.

2 Preliminaries

2.1 Watermarking preliminaries

In wavelet-based watermarking, the watermark embedding can be done prior to compression (also known as uncompressed domain watermarking) or along with compression pipeline as joint compression-watermarking. In the first scenario, the watermark is embedded independent of the compression algorithm. Many examples of this types of watermarking algorithms can be found in the literature [1–13, 25, 26]. The major steps in such an algorithm include the forward DWT (FDWT) and wavelet coefficient modification according to watermark data followed by the inverse DWT (IDWT) to produce the watermarked image. In modern multimedia usage chains, the watermarked image may
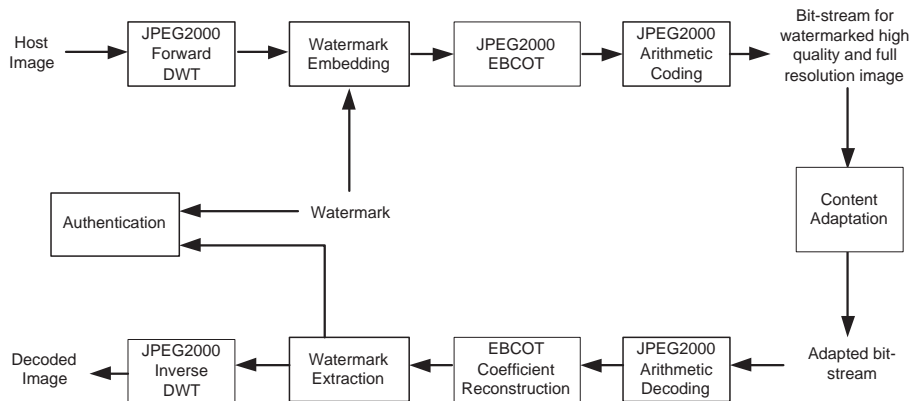
Fig. 1 The proposed watermarking-based authentication scheme in JPEG2000 pipeline.

be scalable coded and adapted to lower quality/resolution versions. Watermark extraction includes the FDWT and recovery of the watermark as a blind or a non-blind extraction algorithm, followed by authentication by comparing with the original watermark.

As JPEG 2000 scalable image coding is based on the DWT, joint compression-watermarking algorithms [14, 16–21] incorporated into JPEG 2000 have also become a more efficient way of image watermarking. In most algorithms, the watermark data is embedded by modifying the quantized wavelet coefficients. This makes such algorithms robust to a given compression level. The watermark is extracted during the image decoding operation. The main difference in joint compression-watermarking algorithms compared to the uncompressed domain algorithms in the context of JPEG 2000-based image consumption framework is that in the latter case there might be a mismatch in the DWT kernel used for watermark embedding and image coding algorithms. This kernel mismatch may be a problem for making them robust for quantization in JPEG 2000 compression. Current joint compression-watermarking algorithms provide a solution for this problem, but they make robust for only for a given compression. They do not address further compression or content adaptation scenarios. Another interesting observation is that the use of JPEG 2000 lossless mode in a joint watermarking-compression scheme is similar to uncompressed-domain watermarking that uses the same DWT kernel for both compression and watermark embedding. That means, if the same DWT kernel is used and the compression is modelled into watermarking, both these types merge into a single framework. An elaborate discussion and an analysis of wavelet-based watermarking algorithms can be found in our previous work [27].

In this paper, we model the effect of compression on watermarked wavelet coefficients, use the model to predict the ability of each un-quantized wavelet coefficient for robustly retaining the watermarked data and rank the un-quantized wavelet coefficients according to this ability. Since the modelling is for un-quantized coefficients, this approach is applicable to both classes of algorithms. The system architecture of the proposed watermarking-based content authentication used within scalable coding is shown in Fig. 1. The embedding process includes three steps: the forward DWT (FDWT), the embedding algorithm that modifies the host wavelet coefficients and the inverse DWT (IDWT). The watermark extraction process includes the FDWT and the recovery of the watermark as a blind or a non-blind extraction. In the proposed scheme the watermark embedding and extraction have been pipelined into the JPEG 2000 encoding and decoding, respectively. Therefore, it avoids unnecessary steps of the IDWT at the watermark embedding and the FDWT at the watermark extraction, thus reducing the complexity.

In the proposed scheme after the FDWT in JPEG 2000, the coefficients are firstly ranked according to the proposed models for non-blind and blind extractions, shown in Section 3 and Section 4, respectively. Subsequently the watermark data is embedded into coefficients chosen according to the rank, by modifying their magnitudes as follows:

$$C'_{m,n} = C_{m,n} + \Delta_{m,n}, \tag{1}$$

where $C_{m,n}$ is the original value of the host wavelet coefficient at the position with (m, n) coordinate indices, $C'_{m,n}$ is the corresponding modified wavelet coefficient and $\Delta_{m,n}$ is the corresponding amount

of modification. In non-blind extraction, since the original copy of the host image is available as reference, the watermark data is usually embedded by directly altering the magnitude of wavelet coefficients [5–16], which can be represented as follows:

$$\Delta_{m,n} = f(\alpha, C_{m,n}^{\beta}, w_{b_{m,n}}),$$
$$= \alpha C_{m,n}^{\beta} w_{b_{m,n}}, \tag{2}$$

where α and β are watermark strength parameters and $w_{b_{m,n}}$ is the watermark embedding value corresponding to the watermark bit b. In blind extraction, since the original copy of the host image is not used in extraction, the modifications have to be referenced to the existing wavelet coefficients themselves. In the most common approach, this is achieved by re-quantizing the host coefficient with respect to two reference coefficients, C_{min} and C_{max}, $i.e.$, the minimum and maximum values in a chosen group [1–4,17]. Following the same form as in Eq. (1), the median coefficient of a group of three coefficients is modified as

$$|\Delta_{m,n}| \leq \delta,$$
$$\text{where } \delta = f(\gamma, C_{min}, C_{max}), \tag{3}$$

where γ is the watermark strength parameter chosen by the user. That means the modification value $\Delta_{m,n}$ is typically a function of the coefficients, C_{min} and C_{max}, for each group of coefficients. The current watermarking literature suggests various functions for computing δ [1,3].

After watermark data is embedded according to the coefficient ranking, they are JPEG 2000 embedded coded using the Embedded Block Coding with Optimal Truncation (EBCOT) followed by arithmetic coding. For non-blind algorithms, since the original image is available for the extraction, the coefficient ranking maps can be reconstructed. Alternatively, as for the blind extraction algorithms, the coefficient ranking data can be sent as auxiliary side information. At the decoder the received portions of the bit stream are entropy decoded and the wavelet coefficients are reconstructed by using the EBCOT reconstruction on the received quality resolution layers. Finally using either the generated or received side information coefficient rank data, the watermark is extracted from the reconstructed wavelet coefficients corresponding to received quality resolution layers. In the following sections we present the proposed models and their use in generating the coefficient ranking maps for the non-blind and blind extraction.

2.2 Quality scalability modeling preliminaries

The resolution-quality layers in the scalable bit stream lead into two types of content enhancement: quality scalability and resolution scalability. The proposed model considers the quality scalability in JPEG 2000 scalable image coding. The simplest form of quality layers used in JPEG 2000 coding corresponds to bit plane-based coding of wavelet coefficients. Choosing certain quality layers up to a certain number of bit planes corresponds to the quantization of the wavelet coefficients. In general, the coefficient quantization due to bit plane discarding, in its simplest form, can be formulated as follows:

$$C_q = \frac{C}{|C|} \left\lfloor \frac{|C|}{Q} \right\rfloor, \tag{4}$$

where C_q is the quantized coefficient, C is the non-zero original coefficient, Q is the quantization factor and $\lfloor x \rfloor$ denotes rounding of x to the largest integer smaller than x (called downward rounding). Embedded quantizers often use $Q = 2^N$, where N is a non-negative integer that corresponds to the number of bit planes being discarded.

At the decoder side, the coefficient reconstruction, often referred to as de-quantization, is represented as multiplying by the quantization factor Q and allowing for the uncertainty due to downward rounding as follows:

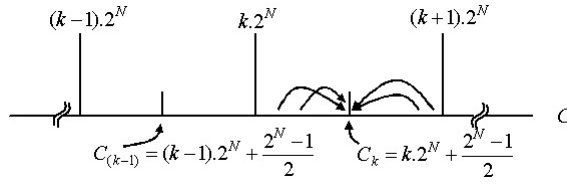$$\hat{C} = C_q Q + \frac{C}{|C|} \left(\frac{Q-1}{2} \right), \tag{5}$$

Fig. 2 The effect of quantization and de-quantization processes in wavelet domain considering discarding of N bit planes.

where $\hat{C}$ is the de-quantized coefficient. The outcome of the combined quantization and de-quantization processes is

$$\hat{C} = \frac{C}{|C|} \left(\left\lfloor \frac{|C|}{Q} \right\rfloor Q + \frac{Q-1}{2} \right). \tag{6}$$

Thereby, one can show that the original coefficient values in the range $kQ \leq C < (k+1)Q$, where $k \in \{0, \pm1, \pm2, ...\}$, are quantized using N bit planes discarding, *i.e.,* $Q = 2^N$, are mapped to $\hat{C} = C_k$, which is the center value of the region marked by kQ and $(k+1)Q$ as shown in Fig. 2. Thus, the center value, C_k, is given by

$$C_k = k2^N + \frac{k}{|k|} \left(\frac{2^N - 1}{2} \right). \tag{7}$$

$N = 0$ correspond to discarding the bit planes corresponding to fractional decimals, *i.e.,* just rounding downwards towards zero. The above relationship in Eq. (7) is further exploited in Section 3 and Section 4, in order to model the watermark robustness to hierarchical bit-plane discarding corresponding to quality layers in JPEG 2000 quality scalable decoding by considering the two extraction scenarios, namely non-blind and blind, respectively.

3 The model for non-blind extraction

For magnitude alteration algorithms we combine Eq. (1) and Eq. (2), ignoring the index subscripts (m, n), to get

$$\begin{aligned} C' &= C + \alpha C w_b, \\ &= C(1 + \alpha w_b), \end{aligned} \tag{8}$$

for the usual case of $\beta = 1$ and $b \in \{0, 1\}$ for a binary watermark logo. The two values, w_0 and w_1, are usually chosen as $w_1 > w_0 > 0$. From Eq. (8), the relationship between C' and C is

$$C = \frac{C'}{1 + \alpha w_b}. \tag{9}$$

Since $(1 + \alpha w_b) > 0$, both C and C' share the same sign. The corresponding modification Δ is

$$\Delta = C' - C = \alpha C w_b. \tag{10}$$

Thus, the extracted watermark value, w'_b, is computed as

$$w'_b = \frac{C' - C}{\alpha C}. \tag{11}$$

Then the recovered watermark value, b', is

$$b' = \begin{cases} 1 &:& w'_b \geq T, \\ 0 &:& w'_b < T, \end{cases} \tag{12}$$

where the threshold $T = \frac{w_0 + w_1}{2}$.

3.1 The Model

Now considering the quantization and de-quantization processes in the compression and decompression, let $\hat{C}'$ be the reconstructed watermarked coefficient after decompression. As shown in Eq. (7) in Section 2.2, for discarding N bit planes, $\hat{C}'$ represents re-mapping of the original watermarked coefficients, C', to the center points, C_k, of the corresponding coefficient cluster, $[k2^N, (k+1)2^N)$, *i.e.,*

$$\hat{C}' = C_k, \quad \forall \quad k2^N \leq C' < (k+1)2^N. \tag{13}$$

The proposed model aims to identify coefficients with magnitude values that fall into regions where the accurate watermark extraction is possible after the quantization and de-quantization processes as follows:

Proposition 1 *The original wavelet coefficients, C, for embedding a bit with value $b = 1$ and retain intact when N bit planes are discarded are in the range*

$$\frac{k.2^N}{1+\alpha w_1} \leq C \leq \frac{C_k}{1+\alpha T},$$

with $k \in \{0, \pm 1, \pm 2, \pm 3, ...\}$.

Proof : To extract $b = 1$ accurately, we need $w_b' \geq T$. That means

$$\frac{C' - C}{\alpha C} \geq T. \tag{14}$$

Since both C' and C share the same sign and $|C'| > |C|$,

$$C' \geq C(1 + \alpha T). \tag{15}$$

If there is no compression, the value of C' is given by Eq. (8). But due to compression, only the reconstructed coefficients, $\hat{C}'$, are available. The correct extraction of $b = 1$ is possible if

$$\hat{C}' \geq C'. \tag{16}$$

Considering the values in the region, $k2^N \leq C' < (k+1)2^N$,

$$\forall \quad k2^N \leq C' \leq C_k, \hat{C}' = C_k \Rightarrow \hat{C}' \geq C',$$
$$\forall \quad C_k < C' < (k+1)2^N, \hat{C}' = C_k \Rightarrow \hat{C}' < C'. \tag{17}$$

Therefore, the condition in Eq. (16) is true when

$$k2^N \leq C' \leq C_k, \tag{18}$$

which in terms of the original coefficients, C, is

$$k2^N \leq C(1 + \alpha w_1) \leq C_k,$$
$$\frac{k2^N}{1+\alpha w_1} \leq C \leq \frac{C_k}{1+\alpha w_1}. \tag{19}$$

However, even if $\hat{C}' < C'$, the correct extraction of $b = 1$ is still possible if (by considering Eq. (15))

$$C_k - C \geq \alpha C T. \tag{20}$$

This means,

$$C_k \geq C(1 + \alpha T),$$
$$C \leq \frac{C_k}{1+\alpha T}. \tag{21}$$

We know that $w_1 > T$. Therefore, $\frac{1}{1+\alpha T} > \frac{1}{1+\alpha w_1}$ and thus we can merge the ranges in Eq. (19) and Eq. (21), as summarized in Fig. 3, to get the range of original coefficients capable of robust extraction of $b = 1$ to

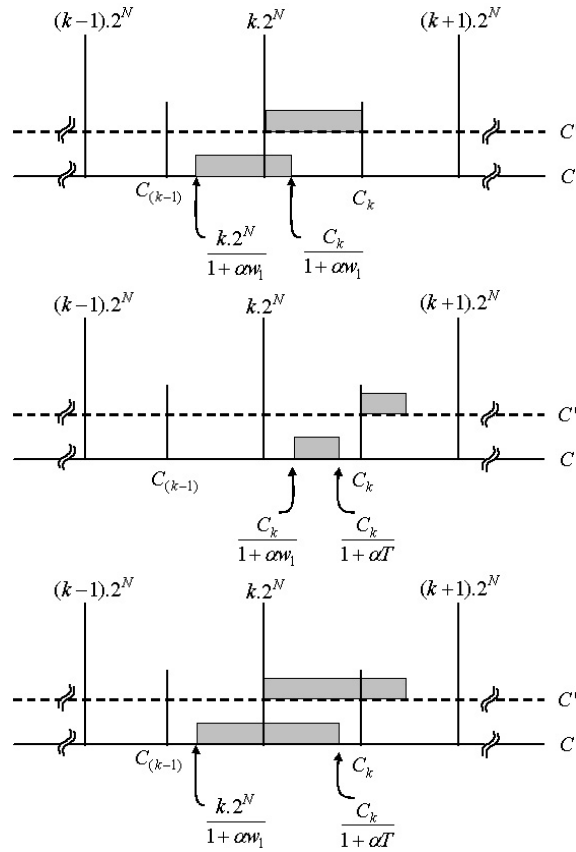$$\frac{k2^N}{1+\alpha w_1} \leq C \leq \frac{C_k}{1+\alpha T}. \tag{22}$$

Fig. 3 The range of C capable of robust extraction of $b = 1$. *Row 1*: $\hat{C}' \geq C'$; *Row 2*: $\hat{C}' < C'$; *Row 3*: The total range.

∎.

Proposition 2 *The original wavelet coefficients, C, for embedding a bit with value $b = 0$ and retain intact when N bit planes are discarded are in the range*

$$\frac{C_{(k-1)}}{1 + \alpha T} < C < \frac{k.2^N}{1 + \alpha w_0},$$

with $k \in \{0, \pm 1, \pm 2, \pm 3, ...\}$.

Proof : To extract $b = 0$ accurately, we need $w_b' < T$. That means

$$\frac{C' - C}{\alpha C} < T, \tag{23}$$
$$C' < C(1 + \alpha T). \tag{24}$$

The correct extraction of $b = 0$ from the reconstructed coefficients, $\hat{C}'$, is possible if

$$\hat{C}' < C'. \tag{25}$$

Therefore, considering the values in the region, $(k - 1)2^N \leq C' < k2^N$,

$$\forall \quad (k-1)2^N \leq C' \leq C_{k-1}, \hat{C}' = C_{k-1} \Rightarrow \hat{C}' \geq C',$$
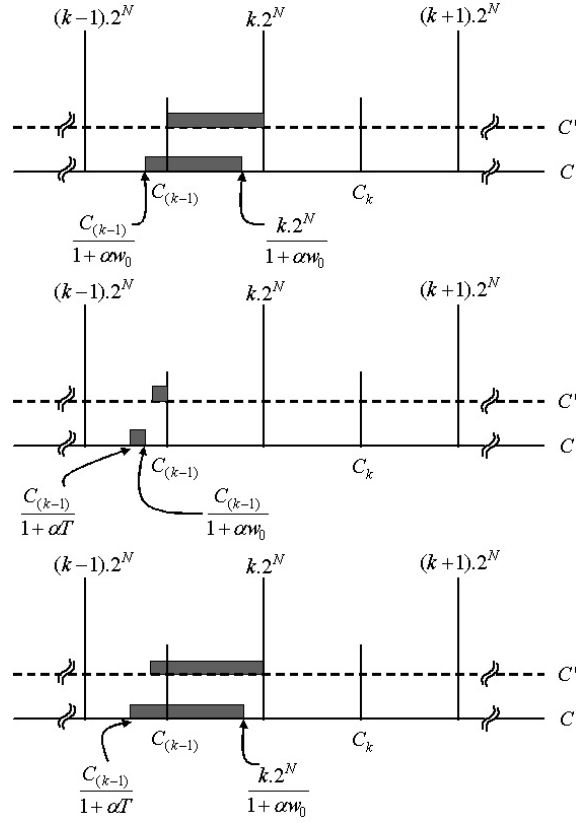$$\forall \quad C_{k-1} < C' < k2^N, \hat{C}' = C_{k-1} \Rightarrow \hat{C}' < C'. \tag{26}$$

Fig. 4 The range of C capable of robust extraction of $b = 0$. *Row 1: $\hat{C}' < C'$; Row 2: $\hat{C}' \geq C'$; Row 3: The total range.*

Therefore, the condition in Eq. (25) is true when

$$C_{k-1} < C' < k2^N, \tag{27}$$

which in terms of the original coefficients, C, is

$$C_{k-1} < C(1 + \alpha w_0) < k2^N,$$
$$\frac{C_{k-1}}{1+\alpha w_0} < C < \frac{k2^N}{1+\alpha w_0}. \tag{28}$$

However, even if $\hat{C}' \geq C'$, the correct extraction of $b = 0$ is still possible if

$$C_{k-1} - C < \alpha C T, \tag{29}$$

as suggested by Eq. (24). This means,

$$C_{k-1} < C(1 + \alpha T),$$
$$C > \frac{C_{k-1}}{1 + \alpha T}. \tag{30}$$

Since $w_0 < T$, we can write $\frac{1}{1+\alpha T} < \frac{1}{1+\alpha w_0}$. Thus we can merge the ranges in Eq. (28) and Eq. (30), as summarized in Fig. 4, to get the range of original coefficients capable of robust extraction of $b = 0$ to

$$\frac{C_{(k-1)}}{1 + \alpha T} < C < \frac{k.2^N}{1 + \alpha w_0}. \tag{31}$$
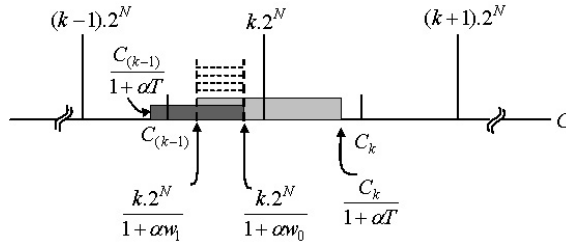
∎.

Fig. 5 The combined range of C capable of robust extraction of both $b = 1$ and $b = 0$.

Finally, as shown in Fig. 5, the above two results in Eq. (22) and Eq. (31) are combined to derive the region of coefficient magnitudes that are capable of retaining both $b = 1$ and $b = 0$ when N bit planes are discarded as follows:

$$\frac{k.2^N}{1 + \alpha w_1} \leq C < \frac{k.2^N}{1 + \alpha w_0}. \tag{32}$$

3.2 Examples

As an example, we choose $w_1 = 0.8$, $w_0 = 0.3$, the threshold $T = 0.55$ and a data set containing coefficient values, C from -512 to 512, and show the ranges of coefficient values that can robustly retain the embedded watermark bits after discarding $N = 7$ bit planes in TABLE 1. Two scenarios of $\alpha = 0.5$ and $\alpha = 0.05$ are shown. First, the coefficient selection for embedding $b = 1$ using Eq. (22) are shown followed by the coefficient selection for embedding $b = 0$ using Eq. (31). Finally the common region is found for embedding any value of b as shown in Eq. (32).

3.3 Ranking maps

This section presents how we use the above derived model to generate the coefficient ranking maps for scalable watermark embedding corresponding to the hierarchical quality layers, which correspond to bit planes. The model considers various values for N, *i.e.*, the number of bit planes being discarded. As an example, we start with $N = 6$ and find the coefficients that are suitable for watermarking under this quantization level. The resulting suitability map consists of two classes, namely, coefficients that are suitable for watermarking in the current quality layer and coefficients that are not suitable

Table 1 Data value (C) ranges for retaining the watermark data, $b = 1$ and $b = 0$ for discarding $N = 7$ bit planes.

(a) $\alpha = 0.5$

	$k \rightarrow$	-5	-4	-3	-2	-1	0	1	2	3	4	5
$b = 1$	min	-512	-460	-358	-256	-153	0	91	183	274	366	457
	max	-457	-366	-274	-183	-91	51	153	256	358	460	512
$b = 0$	min	-512	-445	-334	-223	-111	-51	51	153	256	358	460
	max	-460	-358	-256	-153	-51	0	111	223	334	445	512
$b = 1$ and	min	-512	-445	-334	-223	-111		91	183	274	366	460
$b = 0$	max	-460	-366	-274	-183	-91		111	223	334	445	512

(b) $\alpha = 0.05$

	$k \rightarrow$	-4	-3	-2	-1	0	1	2	3	4
$b = 1$	min	-512	-437	-312	-187	0	123	246	369	492
	max	-492	-369	-246	-123	62	187	312	437	512
$b = 0$	min	-504	-378	-252	-126	-62	62	187	312	437
	max	-437	-312	-187	-62	0	126	252	378	504
$b = 1$ and	min	-504	-378	-252	-126		123	246	369	492
$b = 0$	max	-492	-369	-246	-123		126	252	378	504

for watermarking in the current layer. Then for the next quality enhancement layer, *i.e.,* $N = 5$, we generate a cumulative map with three classes: 1) coefficients that have already been watermarked in the previous quality layers (AW); 2) coefficients that become suitable for watermarking in the current quality layer corresponding to N^{th} bit plane (SW); and 3) coefficients that are not suitable for watermarking yet (NS). For each quality enhancement layer, we update a global ranking map by labeling the S-type coefficients in that quality layer with a unique quality layer number N that corresponds to the associated bit plane discarding as found by the model. This global ranking map can either be sent as auxiliary key information or can be recreated at the decoder using the reference image for non-blind extraction.

Fig. 6 shows the suitability and cumulative maps of wavelet coefficients for the LL subband of a 2-level decomposition for different quality layers corresponding to $N = 6, 5, 4, 3, 2$. In the suitability map white corresponds to suitable coefficients while black corresponds to unsuitable coefficients. In the cumulative maps grey, white and black correspond to AW, SW and NS coefficient classifications, respectively. Fig. 7 shows the global ranking map for LL subband wavelet coefficients of Lena image for 7 quality layers corresponding to $N = 6, 5, 4, 3, 2, 1, 0$ bit planes discarding. White corresponds to coefficients ranked as suitable for $N = 6$ bit plane discarding and black corresponds to coefficients ranked as suitable for $N = 0$ bit plane discarding. The intermediate grey values corresponding to other N values.

4 The model for blind extraction

For the blind extraction, we consider re-quantization-based modification (*e.g.,* [1, 2, 17]), where a group of coefficients (usually three coefficients) is ranked ordered to identify the minimum (C_1), the maximum (C_3) and the median (C_2) coefficients to modify C_2 to obtain C_2' as follows:

$$C_2' = f(\gamma, C_1, C_3, b), \tag{33}$$

where b is binary watermark bit, $b \in \{0, 1\}$, γ is a parameter corresponding to the watermark strength and $f()$ is a non-linear transformation process which is described as follows. This process first partitions the coefficient range, r, where

$$r = C_3 - C_1, \tag{34}$$

by the quantization bin size, δ, defined by

$$\delta = \gamma \frac{|C_1| + |C_3|}{2}, \tag{35}$$

into quantization bins with indexes, $i = 0, 1, ..., \frac{r}{\delta} - 1$. Then in order to embed a watermark bit b, the original value, C_2, is modified to C_2' by choosing any value that comes from the quantization bin index, i, where $b = i\%2$, *i.e.,*

$$C_2' \in \left\{ C : \quad \frac{C - C_1}{\delta} \%2 = b \right\}, \tag{36}$$

where % denotes the modulo operator. To extract the watermark bit, b, back from C_1, C_2' and C_3,

$$b = \left(\frac{C_2' - C_1}{\delta} \right) \%2. \tag{37}$$

4.1 The Model

After compression and decompression, only the reconstructed coefficients, $\hat{C}_1$, $\hat{C}_2'$ and $\hat{C}_3$, are available to the watermark extraction process. In order for the successful extraction, *i.e.,* to maintain the robustness to quality scalable compression, the relationship, $\hat{C}_1 \leq \hat{C}_2' \leq \hat{C}_3$, must be maintained while $\hat{C}_1 \neq \hat{C}_2' \neq \hat{C}_3$ and

$$\hat{b} = \left(\frac{\hat{C}_2' - \hat{C}_1}{\hat{\delta}} \right) \%2, \tag{38}$$

where

$$\hat{\delta} = \gamma \frac{|\hat{C}_1| + |\hat{C}_3|}{2}. \tag{39}$$

As we discussed earlier, the original coefficient values in the range $kQ \leq C < (k+1)Q$, where $k \in \{0, \pm 1, \pm 2, \pm 3, ...\}$ are quantized using N bit plane discarding *i.e.*, $Q = 2^N$, are mapped to $\hat{C} = C_k$, which is the center value of the region marked by kQ and $(k+1)Q$ as shown in Fig. 2. The center value, C_k, of the clusters is given by Eq. (7). In line with this definition, we assume that the mapped three values, $\hat{C}_1$, $\hat{C}'_2$ and $\hat{C}_3$, are C_k, C_{k+m} and C_{k+n}, where $m, n \in \{0, 1, 2, ...\}$ and $0 \leq m \leq n$, respectively as shown in Fig. 8. Therefore, the robustness model needs to estimate the extracted watermark bit, $\hat{b}$, as a function of m, with respect to discarding N bit planes at the time of embedding the watermark.

Proposition 3 *The estimated extracted watermark bit, $\hat{b}$, with respect to discarding N bit planes, is given by*

$$\hat{b} = \left(\frac{2m + y}{\gamma(|k| + |k+n| + 1)} \right) \% 2,$$

where $y = 0$, if C_k and C_{k+m} have the same sign and $y = 2 - 2^{1-N}$, if otherwise.

Proof : C_k in Eq. (7) can be represented in the sign magnitude form as follows:

$$C_k = \frac{k}{|k|} \left(|k|2^N + \frac{2^N - 1}{2} \right). \tag{40}$$

With reference to Eq. (39), the reconstructed watermark quantization step value, $\hat{\delta}$, after discarding N bit planes can now be defined as:

$$\begin{aligned}
\hat{\delta} &= \gamma \frac{|\hat{C}_1| + |\hat{C}_3|}{2}, \\
&= \gamma \frac{|C_k| + |C_{k+n}|}{2}, \\
&= \frac{\gamma}{2} \left(|k|2^N + \frac{2^N - 1}{2} + |k+n|2^N + \frac{2^N - 1}{2} \right), \\
&= \gamma 2^{N-1}(|k| + |k+n| + 1) - \frac{\gamma}{2}, \tag{41}
\end{aligned}$$

The usual values of γ are in the range, $0.05 \leq \gamma \leq 0.1$. Therefore, $\frac{\gamma}{2} << \gamma 2^{N-1}(|k| + |k+n| + 1)$. thus, we can re-write Eq. (41) as

$$\hat{\delta} = \gamma 2^{N-1}(|k| + |k+n| + 1). \tag{42}$$

Using Eq. (40) and Eq. (42) in Eq. (38), the estimated extracted watermark bit, $\hat{b}$, with respect to discarding N bit planes, can be formulated as,

$$\begin{aligned}
\hat{b} &= \left(\frac{\hat{C}_2 - \hat{C}_1}{\hat{\delta}} \right) \% 2, \\
&= \left(\frac{C_{k+m} - C_k}{\hat{\delta}} \right) \% 2, \\
&= \left(\frac{(k+m)2^N + \frac{(k+m)}{|k+m|}\frac{(2^N-1)}{2} - k2^N - \frac{k}{|k|}\frac{(2^N-1)}{2}}{\gamma 2^{N-1}(|k| + |k+n| + 1)} \right) \% 2, \\
&= \left(\frac{m2^N + \left(\frac{(k+m)}{|k+m|} - \frac{k}{|k|} \right) \left(\frac{2^N-1}{2} \right)}{\gamma 2^{N-1}(|k| + |k+n| + 1)} \right) \% 2, \\
&= \left(\frac{2m + \left(\frac{(k+m)}{|k+m|} - \frac{k}{|k|} \right) \left(1 - 2^{-N} \right)}{\gamma(|k| + |k+n| + 1)} \right) \% 2. \tag{43}
\end{aligned}$$

Table 2 Values of m and corresponding $\hat{b}$ for different modifications of C_2' for $k = 1$, $k + n = 6$ and $N = 5$.

C_2' values range	$\hat{C}_2$	m	$\hat{b}$
35-63	47.5	0	0
64-95	79.5	1	1
96-127	111.5	2	1
128-159	143.5	3	0
160-191	175.5	4	0
192-203	207.5	5	1

Now considering the two cases: k and $k+m$ have the same sign (Case 1) and k and $k+m$ have different signs (Case 2),

$$\hat{b} = \begin{cases} \left(\frac{2m}{\gamma(|k|+|k+n|+1)} \right) \%2 & : \quad \text{Case 1}, \\ \left(\frac{2m+2-2^{1-N}}{\gamma(|k|+|k+n|+1)} \right) \%2 & : \quad \text{Case 2}. \end{cases} \tag{44}$$

$\blacksquare$.

Thus, using Eq. (44), it is possible to predict $\hat{b}$ for a given number of discarded bit planes, N, for particular modifications of C_2 to C_2' during embedding. This relationship is used for identifying the ranges of values for C_2', *i.e.*, the value of C_2 after embedding the watermark bit, b, by considering the value of m for given k, n and N. Similarly the optimal values of C_2' for other $N - t$, where $t \in \{1, 2, 3...N - 1\}$ lower bit-planes being discarded are calculated to maintain the robustness for discarding of any bit plane up to the Nth bit plane.

4.2 Examples

Let $C_1 = 35$, $C_2 = 181$ and $C_3 = 203$ be the three coefficients concerned. Set $\gamma = 0.1$ and consider $N = 5$ bit planes are being discarded. Then $k = \lfloor 35/2^N \rfloor = \lfloor 35/2^5 \rfloor = \lfloor 35/32 \rfloor = 1$ and $k + n = \lfloor 203/2^5 \rfloor = \lfloor 203/32 \rfloor = 6$. Thus, Eq. (44) is simplified to $\hat{b} = (2.5m)\%2$. A look-up table, as shown in TABLE 2, of $\hat{b}$ for different $\hat{C}_2$ and corresponding m is derived. Thus, in this example, for robustly embedding a watermark bit, $b = 0$, C_2 can be modified to any value in the regions, $35 \leq C_2' \leq 63$ and $128 \leq C_2' \leq 191$. Similarly, for robustly embedding a watermark bit, $b = 1$, C_2 can be modified to any value in the regions, $64 \leq C_2' \leq 127$ and $192 \leq C_2' \leq 203$. However, a value close to the original value, C_2, within these ranges is chosen in order to minimize the amount of distortion.

Similar computations are carried out for $N = 1, 2, 3, 4...$ to obtain the corresponding robust ranges for C_2' The common range for all N values ensures correct watermark extraction when N or any lower number of bit planes are discarded. The extension of our previous example for $N = 1, 2, 3, 4$ to find the value ranges of C_2' to embed the watermark bits, $b = 1$ or $b = 0$, is shown in TABLE 3.

4.3 Ranking maps

Using the proposed model for blind extraction, we generate the suitability maps and cumulative maps for each quality layers corresponding to different N bit plane discarding scenarios as shown in Section 3.3. For the blind extraction we choose 3 coefficients corresponding to the same spatial location in three high frequency subbands, HL, LH and HH. The suitability and cumulative maps for the spatial locations considering the first level of decomposition are shown in Fig. 9. Fig. 10 shows the global ranking maps for high frequency subband spatial locations for three levels of wavelet decomposition of Lena image for 7 quality layers corresponding to $N = 6, 5, 4, 3, 2, 1, 0$ bit planes discarding. White corresponds to coefficients ranked as suitable for $N = 6$ bit plane discarding and black corresponds to coefficients ranked as suitable for $N = 0$ bit plane discarding. The intermediate grey values corresponding to other N values.

Table 3 Ranges of C_2' to embed watermark bits, $b = 1$ and $b = 0$, for different N

	Embedding $b = 0$	
	Robustness for discarding N bit planes	Robustness for discarding up to N bit planes
$N = 1$	172-184 & 196-208	-
$N = 2$	168-180 & 192-204	172-180 & 196-204
$N = 3$	176-184 & 200-208	176-180 & 200-204
$N = 4$	176-192 & 224-240	176-180
$N = 5$	128-192	176-180
	Embedding $b = 1$	
	Robustness for discarding N bit planes	Robustness for discarding up to N bit planes
$N = 1$	160-172 & 184-196	-
$N = 2$	156-168 & 180-192	160-168 &184-192
$N = 3$	160-176 & 184-200	160-176 &184-192
$N = 4$	144-176 & 192-224	160-176
$N = 5$	192-256	-

5 Verification of the proposed models

This section presents the results of experimental verification of the proposed two models by simulating wavelet domain bit plane discarding corresponding to quality scalability. In the experiments, firstly the watermark data is embedded by considering different values of N, *i.e.,* the maximum number of bit planes that can be discarded without affecting the accuracy of extraction. Then for each case of N, the robustness to different quality scalable decoding scenarios using different quantization factors, Q, where $Q = 2^p$ and p is the corresponding number of bit planes being discarded for quality scalability, is evaluated. The extracted watermark data is compared with the original watermark data by comparing the Hamming distance, which is also another form of bit error rate (BER) measurement. The lower the Hamming distance, the higher the accuracy of extraction, thus high robustness.

The proposed model for non-blind watermarking is evaluated using the magnitude alteration algorithm presented in [12] as the control algorithm. The proposed model is incorporated into the algorithm in [12] for generating the global rank map of the coefficients for embedding the watermark. Then the extraction accuracy for quality scalability is compared with that of the original algorithm that does not use the proposed model under various quality scalability scenarios, e.g., starting from $p = 6$ and gradually enhancing quality for decreasing p. The experimental setup includes the 9/7 wavelet, 3 levels of decomposition and embedding within the LL frequency subband using $\alpha = 0.01$.

Similarly, we use the blind watermarking scheme presented in [1] as the control algorithm to verify the model proposed for blind watermarking algorithms. The experimental setup includes the 9/7 wavelet, 3 levels of decomposition and embedding using $\gamma = 0.02$ within the high frequency subband coefficients from a single level decomposition. In both cases, model-based embedding considers different starting values of N, *i.e.,* the maximum number of bit planes that can be discarded without affecting the accuracy.

Fig. 11 and Fig. 12 show verification of the non-blind model and blind model, respectively. They compare the Hamming distance of extracted watermark data that have been embedded using the proposed model with different maximum number of bit planes to be discarded (N) against the case of without using the model for different number (p) of actual bit planes being discarded at the decoder for four different images: Lena, Barbara, Gold Hill and Boats. From the plots in both figures it is evident that the extraction accuracy remains high for any $p \leq N$, *i.e.,* when the number of bit planes being actually discarded is smaller than or equal to the maximum value of N considered in the model. This verifies the correct performance of the model and the high robustness to various bit plane discarding levels.

6 Performance Evaluation

In this section we present the performance of the proposed scalable watermark extraction that utilizes the scalable decoding functionality of JPEG 2000. The proposed models in previous sections address

the quality scalability of JPEG 2000. In order to address the resolution scalability, before embedding the watermark logo, we partition it into segments and different segments are embedded within different wavelet decomposition levels. If the segment spread is made known to the extractor as a key with auxiliary information, the watermark extraction can be made scalable to resolution scalability of the JPEG 2000 coded images. Finally, JPEG 2000 quality scalability and resolution scalability-based extraction experiments are performed using our watermark evaluation bench for content adaptation modes (WEBCAM) framework [27, 28] to evaluate the performance of the proposed models in actual quality-resolution scalability scenarios.

Firstly, in order to demonstrate scalable extraction, we embed watermarking data using the model considering $N = 6$ maximum number of bit plane discarding and show in Fig. 13 the percentages of watermark bits extraction when the quality is enhanced. We start with $p = 6$ bit planes being discarded and reducing the number of bit planes being discarded by 1 till it becomes $p = 0$. Left column shows the non-blind model performance and right column shows the blind column performance for the four test images. For both models, the plots show the increasing number of extractions, thus the increasing complexity of the authentication process with the quality enhancements. Similarly, the scalable extraction complexity performance with respect to JPEG 2000 quality scalability starting from 32:1 compression and enhancing quality to compression ratios, 24:1, 16:1, 8:1, 4:1 and 2:1 considering three levels of resolution scalability (quarter resolution, half resolution and full resolution) for both models for Lena image is shown in Fig. 14.

The authentication performance of the proposed methodology using the two models are shown in Fig. 15 and Fig. 16. For non-blind methods, we also compare the proposed model with another pixel masking model that uses the human visual system aspects for efficient wavelet-based watermarking [9]. For fair comparison, we use the same coefficient modification method for obtaining the results shown in all three plots in these figures. For blind-methods, we have considered the joint compression-watermarking algorithm presented in [17] and compare its performance without using any model and with using the proposed model. We also compare with another wavelet-based quanitization-based algorithm presented in [3]. In all cases, the plots demonstrate the superior performance of the proposed models resulting in very low Hamming distances. Further with more and more bits extracted when the host image quality is enhanced, thus resulting in scalability. For example, a very low Hamming distance can be achieved only by decoding a stream up to compression ratios of 32:1 (for non-blind case) or 24:1 (for blind case), *i.e.,* only extracting about 10% of the total logo. The scalable authentication of the proposed scheme can be demonstrated by taking the ratio of Hamming distances in Fig. 15 to the extracted logo percentages in the corresponding compression ratios in the left column plots in Fig. 14 for non-blind extractions. This ratio becomes smaller when the compression ratio is reduced, *i.e.,* when updated more quality layers. However, for the existing watermark extraction algorithms, that do not utilize the quality scalable decoding and the proposed model to compute the Hamming distance, one has to extract all watermarked data as it is not possible to know which watermark bits were received first or which were affected due to quality discarding or enhancements. A similar relationship can be observed comparing Fig. 16 with the right column plots in Fig. 14 for blind extractions.

We further demonstrate the advantage of the proposed scheme by comparing the extracted logos under different compression ratios with increasing quality and resolution enhancements for both with the model and without the model. Fig. 17, Fig. 18 and Fig. 19 show the scalable extraction of logo data with increasing quality enhancements corresponding to various compression ratios (CR) for 3 resolution scalability layers of the host image Lena, respectively. The top row shows the logo reconstruction for existing algorithms, that do not use the proposed model, while the bottom rom shows the result for the proposed model. In these figures for the proposed model, since the extraction algorithm knows exactly which watermark bits are extracted at a given resolution-quality layer, the non-relevant locations are marked in gray in the extracted logos to indicate the scalable extraction. It is evident from these reconstructed logos the scalability and the higher accuracy of the extraction process. Similarly, the scalable watermark logo reconstruction for blind extraction and its comparison with existing algorithm not using the model are shown in Fig. 20, Fig. 21 and Fig. 22. All these figures show the scalable extraction and authentication of the work proposed in this paper.

7 Conclusions

In this paper we have presented a scalable watermark embedding and extraction method for fast, scalable and low complexity authentication of JPEG 2000 images leading to real-time operations. We proposed novel models for estimating the coefficients' ability to retain watermark information intact under the embedded quantization corresponding to various quality enhancement in JPEG 2000 scalable coding and decoding for both blind and non-blind extraction. Using the model, the embedding algorithm generates a global ranking map of suitable wavelet coefficients for watermark embedding that supports scalable extraction. The simulations verifies the superior performance of the proposed models under quality scalability scenarios compared to the performance of algorithms that do not use such a model *i.e.,* not considering the quality scalability functionality of JPEG 2000 bit streams. The performance, in terms of Hamming distance and the quality of the reconstructed watermark logo, of the proposed methodology is much better than other exiting algorithms which do not consider the quality and resolution scalability in JPEG 2000. At the decoder when more and more quality and resolution layers are decoded the authentication metric is improved, thus resulting in gradually increasing complexity of the authentication process according to the number of quality and resolution enhancements. The low complexity authentication is available at low quality low resolution decoding, enabling real-time authentication for resource constrained applications without affecting the authentication metric. Compared to the existing methods, the proposed method results in fast, low complexity, highly robust and scalable authentication of JPEG 2000 coded images.

Acknowledgement

References

1. L. Xie and G. R. Arce, "Joint wavelet compression and authentication watermarking," in *Proc. IEEE ICIP*, vol. 2, 1998, pp. 427–431.
2. F. Huo and X. Gao, "A wavelet based image watermarking scheme," in *Proc. IEEE ICIP*, 2006, pp. 2573–2576.
3. D. Kundur and D. Hatzinakos, "Digital watermarking using multiresolution wavelet decomposition," in *Proc. IEEE ICASSP*, vol. 5, 1998, pp. 2969–2972.
4. C. Jin and J. Peng, "A robust wavelet-based blind digital watermarking algorithm," *Information Technology Journal*, vol. 5, no. 2, pp. 358–363, 2006.
5. H. Tao, J. Liu, and J. Tian, "Digital watermarking technique based on integer Harr transforms and visual properties," in *Proc. SPIE Image Compression and Encryption Tech.*, vol. 4551, no. 1, 2001, pp. 239–244.
6. X. Xia, C. G. Boncelet, and G. R. Arce, "Wavelet transform based watermark for digital images," *Optic Express*, vol. 3, no. 12, pp. 497–511, Dec. 1998.
7. X. C. Feng and Y. Yang, "A new watermarking method based on DWT," in *Proc. Int'l Conf. on Computational Intelligence and Security, Lect. Notes in Comp. Sci. (LNCS)*, vol. 3802, 2005, pp. 1122–1126.
8. Q. Gong and H. Shen, "Toward blind logo watermarking in JPEG-compressed images," in *Proc. Int'l Conf. on Parallel and Distributed Comp., Appl. and Tech., (PDCAT)*, 2005, pp. 1058–1062.
9. M. Barni, F. Bartolini, and A. Piva, "Improved wavelet-based watermarking through pixel-wise masking," *IEEE Trans. Image Processing*, vol. 10, no. 5, pp. 783–791, May 2001.
10. D. Kundur and D. Hatzinakos, "Toward robust logo watermarking using multiresolution image fusion principles," *IEEE Trans. Multimedia*, vol. 6, no. 1, pp. 185–198, Feb. 2004.
11. Z. Zhang and Y. L. Mo, "Embedding strategy of image watermarking in wavelet transform domain," in *Proc. SPIE Image Compression and Encryption Tech.*, vol. 4551, no. 1, 2001, pp. 127–131.
12. J. R. Kim and Y. S. Moon, "A robust wavelet-based digital watermarking using level-adaptive thresholding," in *Proc. IEEE ICIP*, vol. 2, 1999, pp. 226–230.
13. S. Marusic, D. B. H. Tay, G. Deng, and P. Marimuthu, "A study of biorthogonal wavelets in digital watermarking," in *Proc. IEEE ICIP*, vol. 3, Sept. 2003, pp. II–463–6.
14. T.-S. Chen, J. Chen, and J.-G. Chen, "A simple and efficient watermarking technique based on JPEG2000 codec," in *Proc. Int'l Symp. on Multimedia Software Eng.*, 2003, pp. 80–87.
15. F. Dufaux, S. J. Wee, J. G. Apostolopoulos, and T. Ebrahimi, "JPSEC for secure imaging in JPEG2000," in *Proc. SPIE Appl. of Digital Image Processing XXVII*, vol. 5558, no. 1, 2004, pp. 319–330.
16. Y.-S. Seo, M.-S. Kim, H.-J. Park, H.-Y. Jung, H.-Y. Chung, Y. Huh, and J.-D. Lee, "A secure watermarking for JPEG2000," in *Proc. IEEE ICIP*, vol. 2, 2001, pp. 530–533.

17. P. Meerwald, "Quantization watermarking in the JPEG2000 coding pipeline," in *Proc. Int'l Working Conf. on Comms. and Multimedia Security*, 2001, pp. 69–79.

18. Q. Sun and S. Chang, "A secure and robust digital signature scheme for JPEG2000 image authentication," *IEEE Trans. Multimedia*, vol. 7, no. 3, pp. 480–494, June 2005.

19. R. Grosbois, P. Gerbelot, and T. Ebrahimi, "Authentication and access control in the JPEG2000 compressed domain," in *Proc. SPIE Appl. of Digital Image Processing XXIV*, vol. 4472, no. 1, 2001, pp. 95–104.

20. M. A. Suhail, M. S. Obaidat, S. S. Ipson, and B. Sadoun, "A comparative study of digital watermarking in JPEG and JPEG2000 environments," *Information Sciences*, vol. 151, pp. 93–105, 2003.

21. R. Grosbois and T. Ebrahimi, "Watermarking in the JPEG 2000 domain," in *Proc. IEEE MMSP*, 2001, pp. 339 –344.

22. D. S. Taubman and M. W. Marcellin, *JPEG2000 Image Compression Fundamentals, Standards and Practice*. USA: Springer, 2002.

23. T. Ebrahimi and R. Grosbois, "Secure JPEG 2000-JPSEC," in *Proc. IEEE ICASSP*, vol. 4, 2003, pp. 716–719.

24. D. Bhowmik and C. Abhayaratne, "Evaluation of watermark robustness to JPEG2000 based content adaptation attacks," in *Proc. IET Int'l Conf. on Visual Info. Eng. (VIE '08)*, 2008, pp. 789–794.

25. P. Campisi, "Video watermarking in the 3D-DWT domain using quantization-based methods," in *Proc. IEEE MMSP*, 2005, pp. 1–4.

26. P. Meerwald and A. Uhl, "A survey of wavelet-domain watermarking algorithms," in *Proc. SPIE Security and Watermarking of Multimedia Contents III*, vol. 4314, 2001, pp. 505–516.

27. D. Bhowmik and C. Abhayaratne, "A framework for evaluating wavelet based watermarking for scalable coded digital item adaptation attacks," in *Proc. SPIE Wavelet Appl. in Industrial Processing VI*, vol. 7248, no. 1, 2009, p. 72480M (10 pages).

28. ——. Watermarking Evaluation Bench for Content Adaptation Modes (WEBCAM). [Online]. Available: http://svc.group.shef.ac.uk/webcam.html [Accessed: Jan. 2010].

Charith Abhayaratne

Charith Abhayaratne received the B.E, in Electrical and Electronic Engineering from the University of Adelaide in Australia in 1998 and the Ph.D. in Electronic and Electrical Engineering from the University of Bath in 2002. Since July 2005, he has been a lecturer within the Department of Electronic and Electrical Engineering at the University of Sheffield in United Kingdom. He was a recipient of European Research Consortium for Informatics and Mathematics (ERCIM) postdoctoral fellowship in 2002-2003 to carry out research at the Centre for mathematics and computer science (CWI) in Amsterdam in the Netherlands and at the National Research Institute for computer science and control (INRIA) in Sophia Antipolis in France. From 2004-2005, Dr Abhayaratne was with the Multimedia and Vision laboratory of the Queen Mary, University of London as a senior research officer. His research interests include wavelets and signal transforms, video and image compression, visual analysis and visual content identification. He has contributed to MPEG on scalable video coding standardization and wavelet video exploration. He has been a reviewer for leading IEEE/IET/ACM/SPIE journals and conferences, UK Engineering and Physical Science Research council (EPSRC) and book publishers. He has been involved in technical programme committees for several leading international conferences and served as session chairs. He co-chaired the international workshop on "Scalable coded media beyond compression" as part of the IET VIE'08 conference. Dr Abhayaratne is the United Kingdom's liaison officer for the European Association for Signal Processing (EURASIP).

Deepayan Bhowmik

Deepayan Bhowmik received the Ph.D. in Electronic and Electrical Engineering from The University of Sheffield in 2011. Prior to that, he received the B.Eng in Electronic Engineering from Visvesvaraya National Institute of Technology, Nagpur, India in 2003 and the M.Sc. in Electronic and Information Technology from Sheffield Hallam University, UK in 2006. Currently, he is working as a postdoctoral research assistant in the Department of Electronic and Electrical Engineering at the University of Sheffield, UK. His research interests include image and video watermarking.
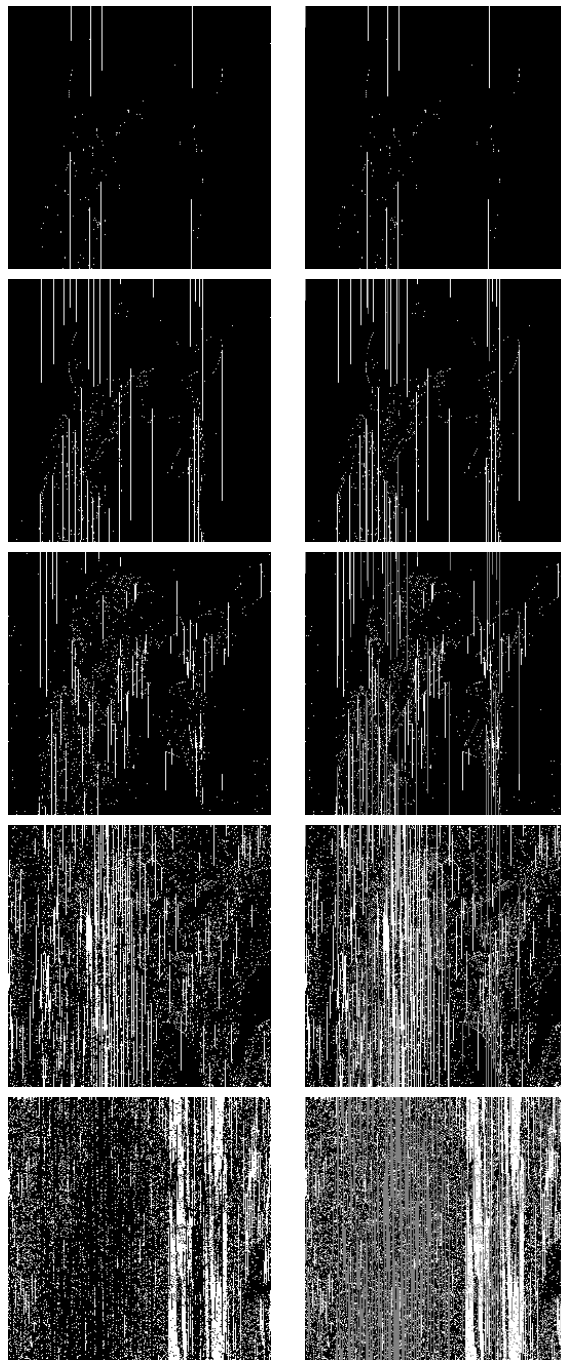
Fig. 6 LL subband coefficients' suitability maps (left column) and cumulative maps (right column) for non-blind extraction for quality layers corresponding to discarding of $N = 6, 5, 4, 3, 2$ bit planes (from top row to bottom row, respectively). Suitability maps - white and black correspond to suitable and not suitable for watermarking, respectively. Cumulative maps - gray, white and black correspond to AW, SW and NS coefficient types, respectively.
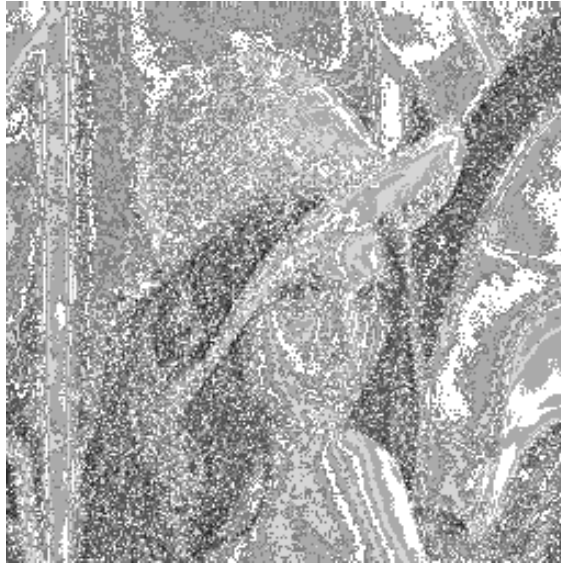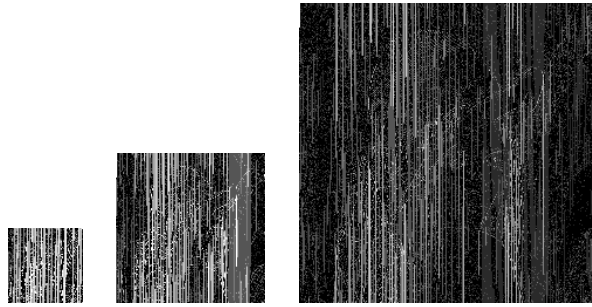
Fig. 7 LL subband coefficients' global ranking map for 7 quality layers corresponding to $N = 6, 5, 4, 3, 2, 1, 0$ bit planes discarding represented in the gray scale with $N = 6$ shown in white and $N = 0$ shown in black.
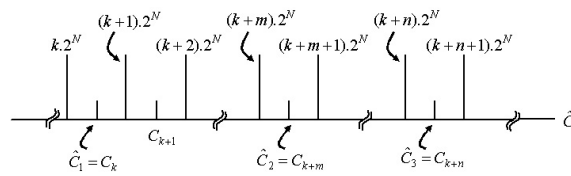

Fig. 8 Mapping of coefficients after quantization and de-quantization processes considering the discarding of N bit planes.

Fig. 9 Suitability maps (left column) and cumulative maps (right column) for blind extraction for quality layers corresponding to discarding of $N = 5, 4, 3, 2, 1$ bit planes (from top row to bottom row, respectively). Suitability maps - white and black correspond to suitable and not suitable for watermarking, respectively. Cumulative maps - gray, white and black correspond to AW, SW and NS coefficient types, respectively.

Fig. 10 Blind extraction high frequency subband spatial location global ranking maps for third, second and first levels of wavelet decomposition for 7 quality layers corresponding to $N = 6, 5, 4, 3, 2, 1, 0$ bit planes discarding represented in the gray scale with $N = 6$ shown in white and $N = 0$ shown in black.
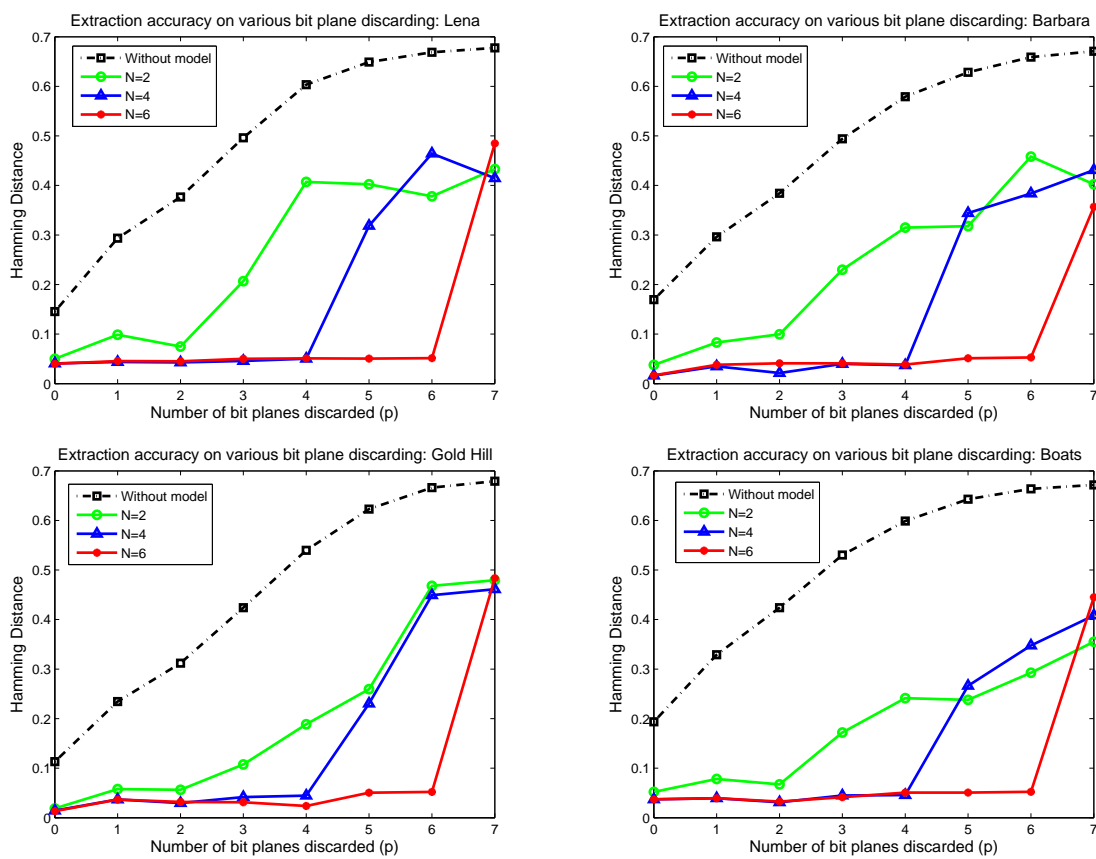
Fig. 11 Non-blind model verification using 4 different host images: Extraction accuracy against discarding of p bit planes.
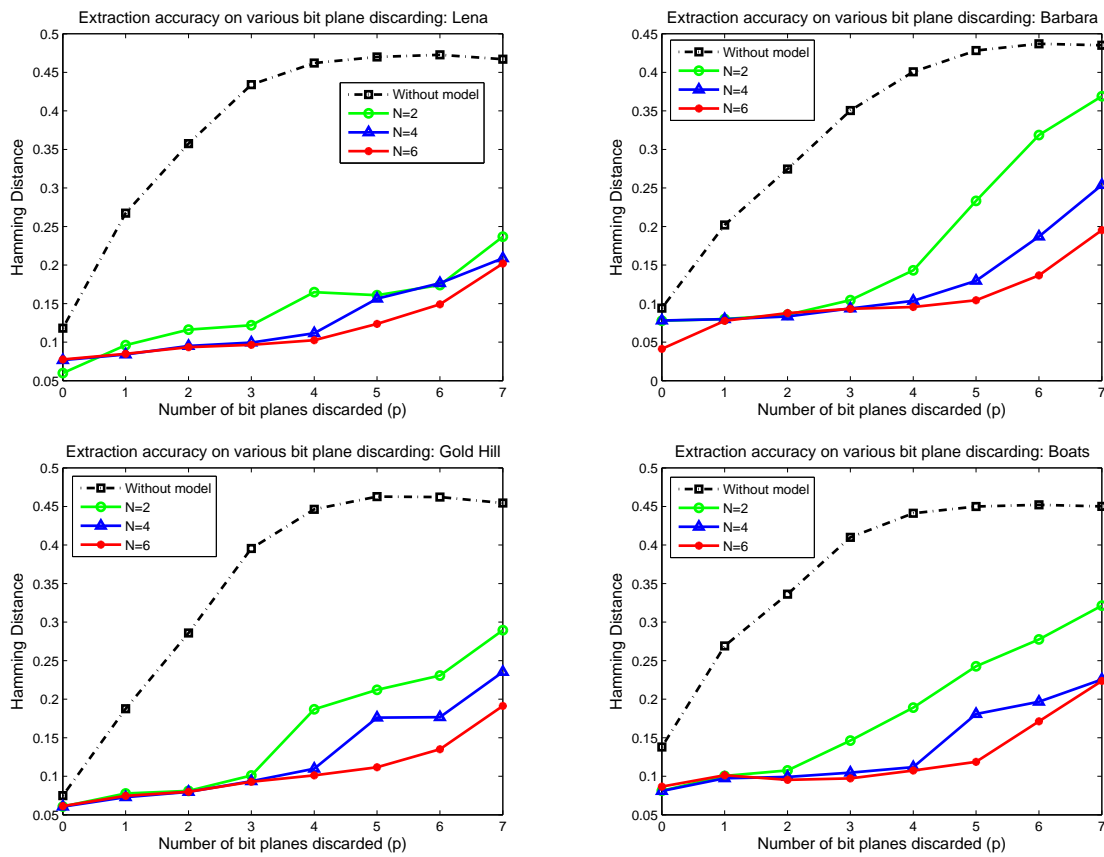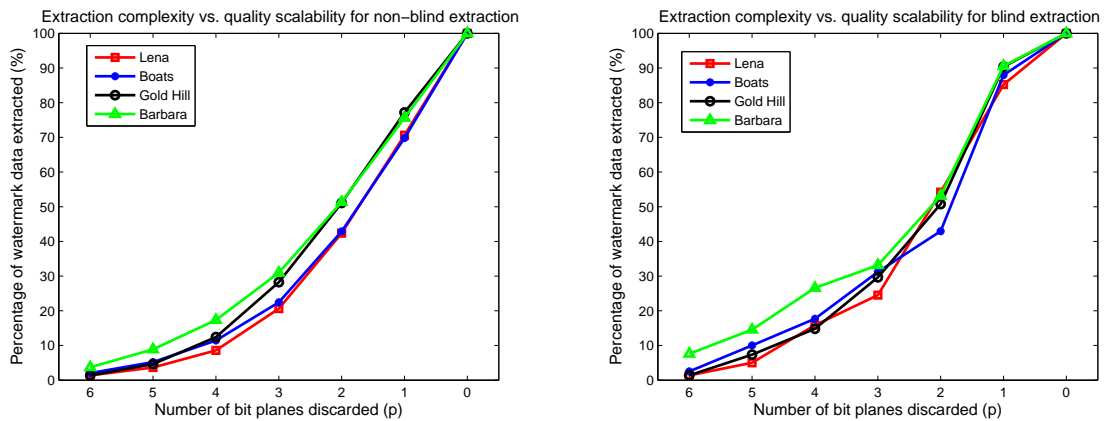
Fig. 12 Blind model verification using 4 different host images: Extraction accuracy against discarding of p bit planes.

Fig. 13 Scalable watermark extraction against quality enhancements by reducing the number of bit planes being discarded (p). Left column shows the non-blind model performance and right column shows the blind column performance
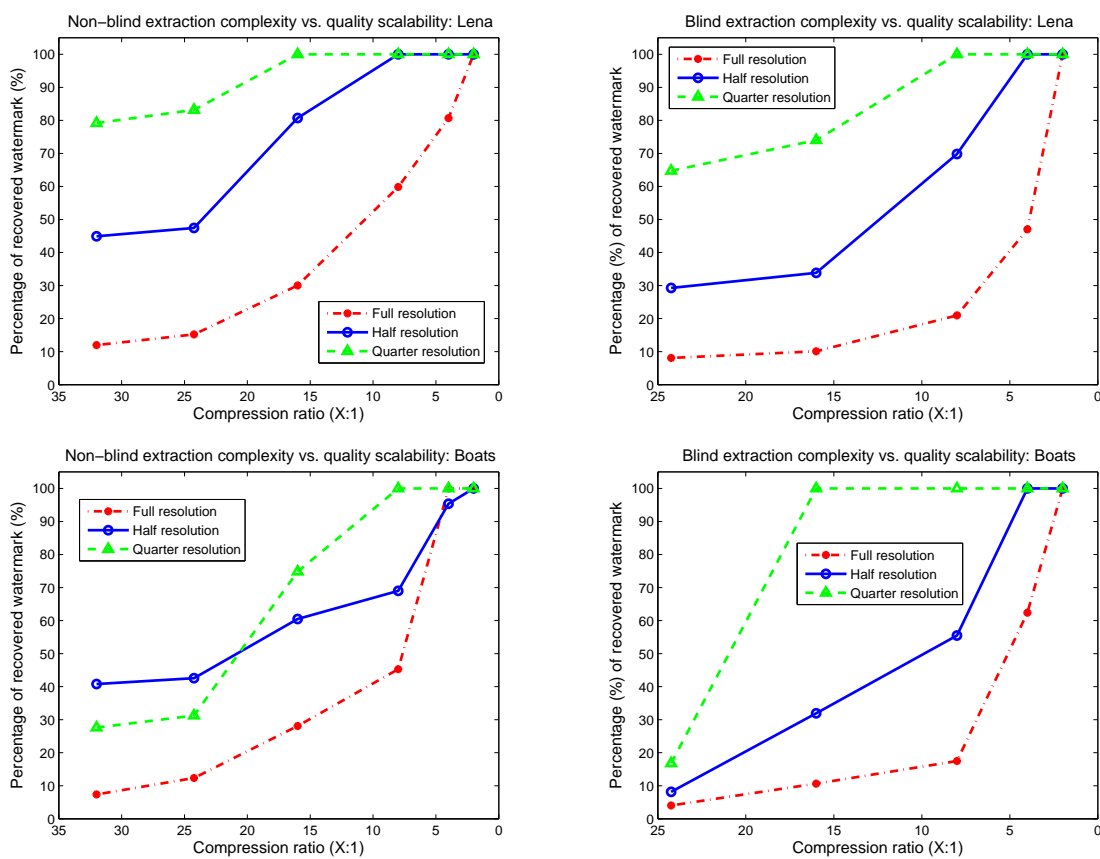
Fig. 14 Scalable watermark extraction against quality enhancements by JPEG 2000 decoding for different resolutions. Left column shows the non-blind model performance and right column shows the blind column performance
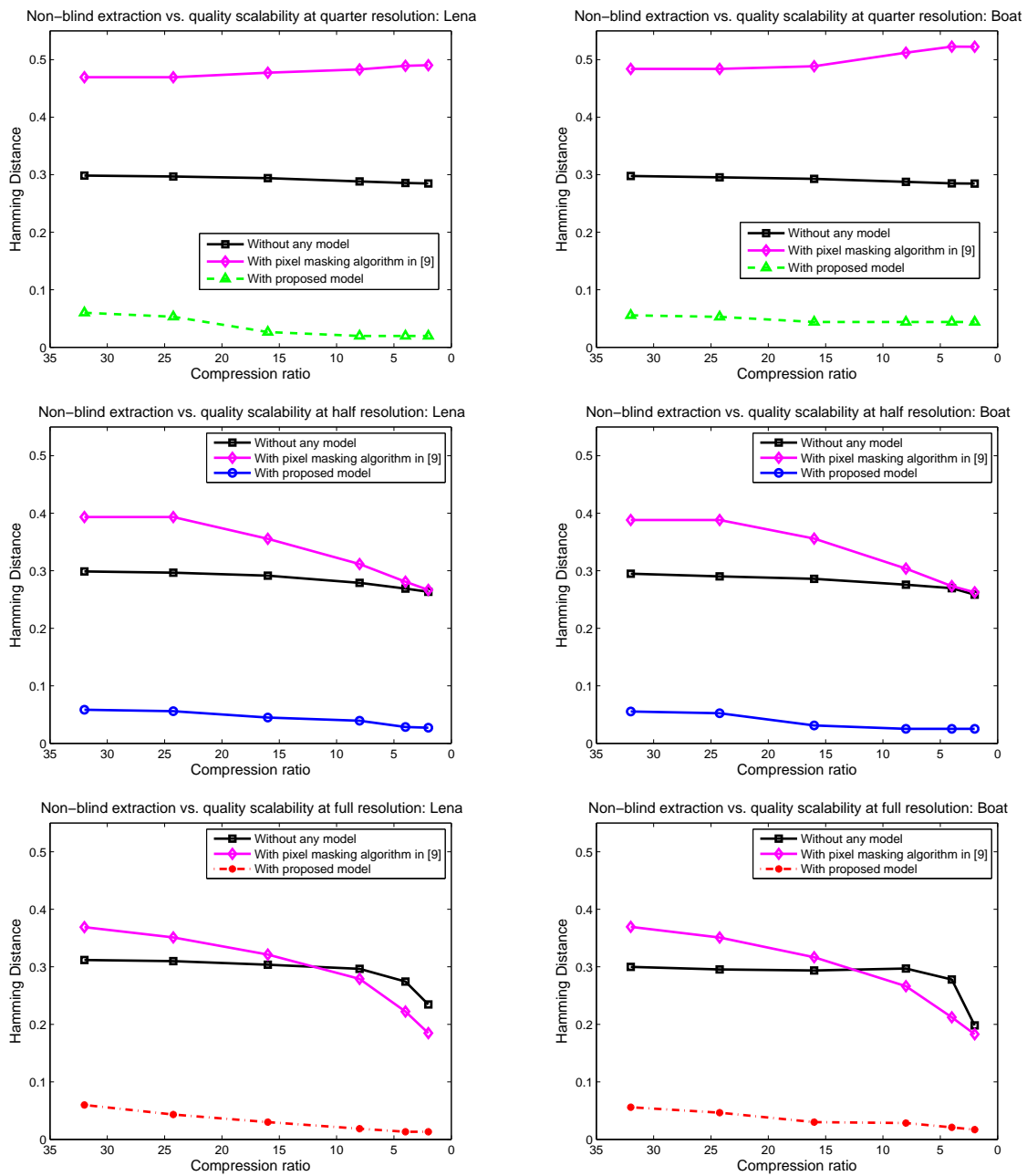
Fig. 15 Non-blind scalable watermark authentication against quality enhancements by JPEG 2000 decoding for different resolutions: quarter (top row), half (middle row) and full (bottom row) for two host images Lena (left column) and Boats (right column)
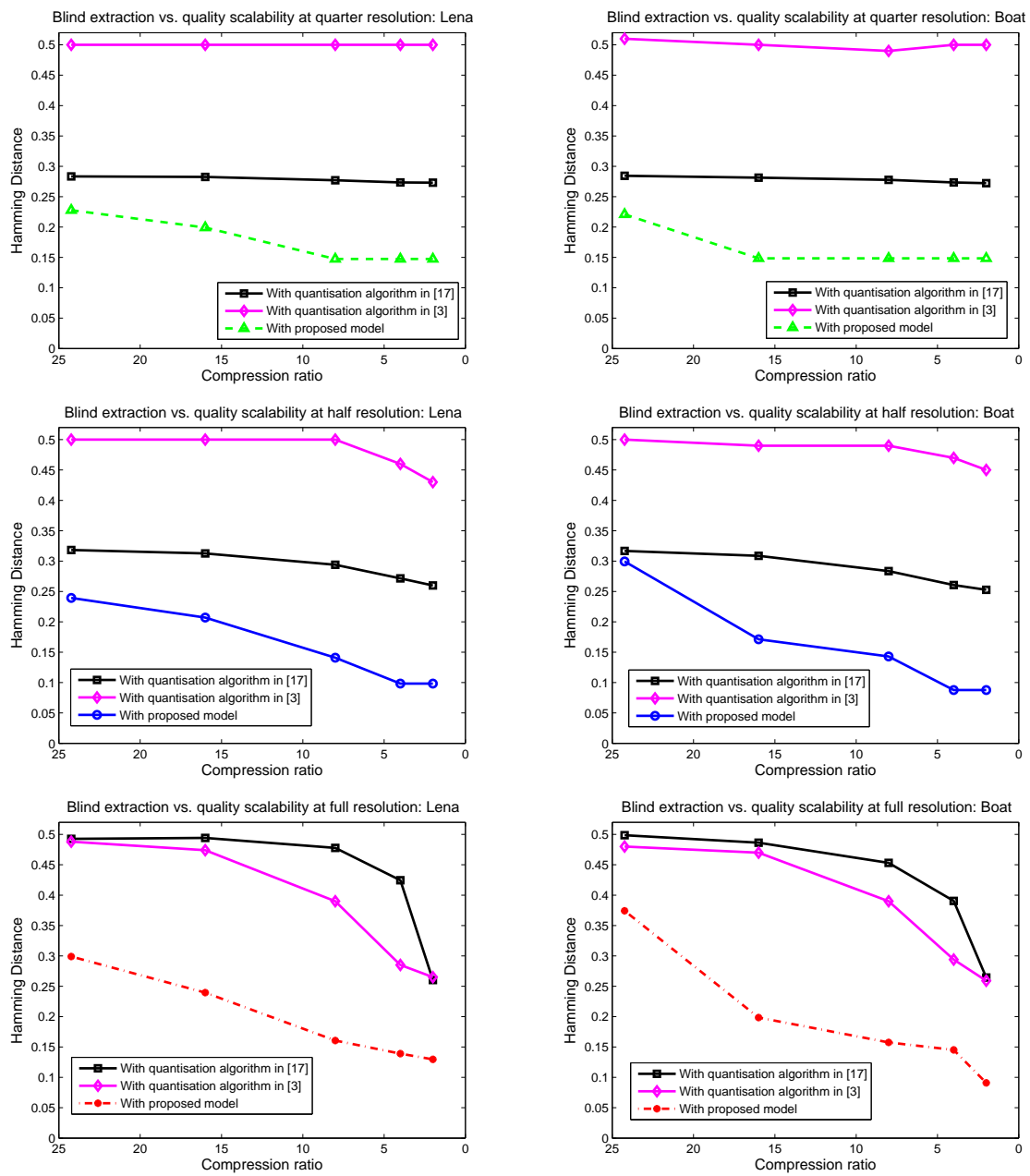
Fig. 16 Blind scalable watermark authentication against quality enhancements by JPEG 2000 decoding for different resolutions: quarter (top row), half (middle row) and full (bottom row) for two host images Lena (left column) and Boats (right column)
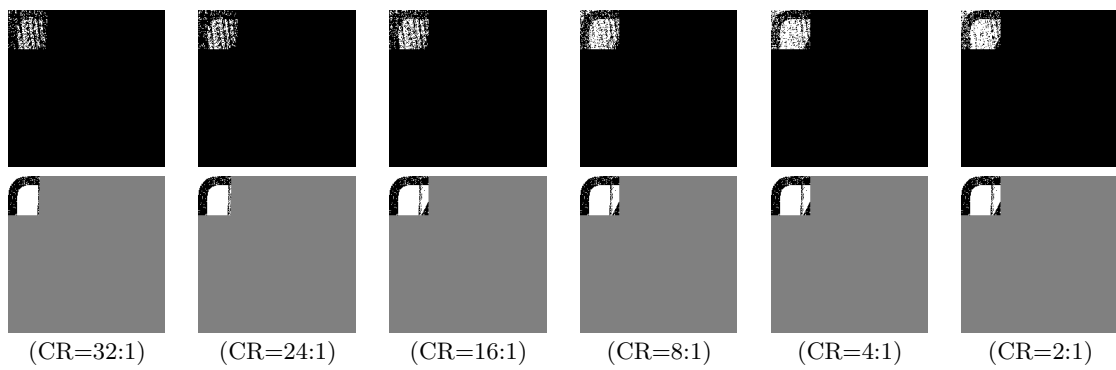
| | | | | | |
| (CR=32:1) | (CR=24:1) | (CR=16:1) | (CR=8:1) | (CR=4:1) | (CR=2:1) |

Fig. 17 Extracted watermark logo for JPEG 2000 quality scalability for quarter resolution scalability using non-blind extraction. *Row 1:* Without the model and *Row 2:* With the proposed model.
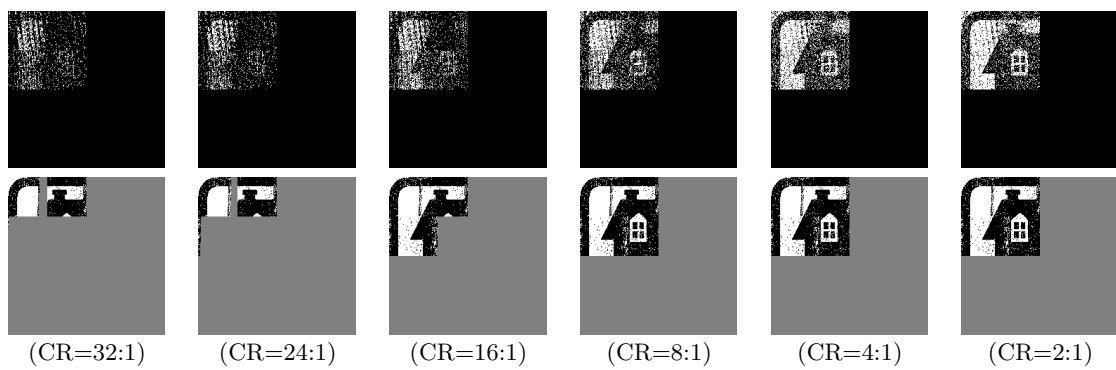

| | | | | | |
| (CR=32:1) | (CR=24:1) | (CR=16:1) | (CR=8:1) | (CR=4:1) | (CR=2:1) |

Fig. 18 Extracted watermark logo for JPEG 2000 quality scalability for half resolution scalability using non-blind extraction. *Row 1:* Without the model and *Row 2:* With the proposed model.
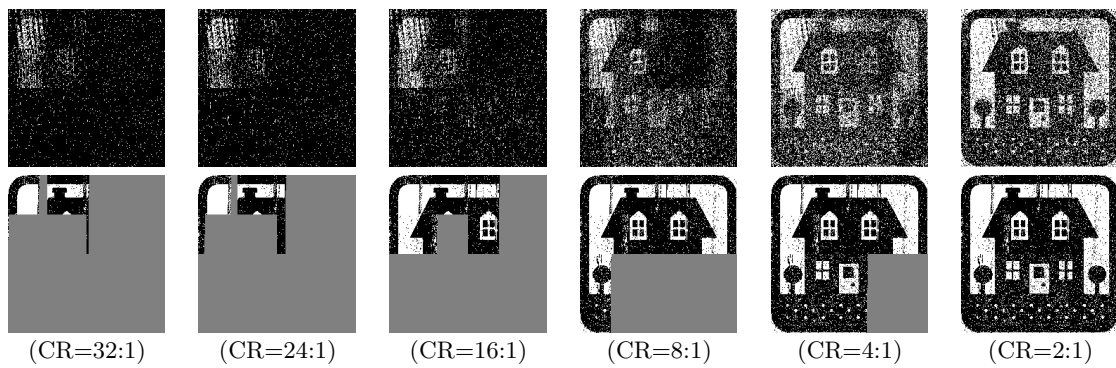

| | | | | | |
| (CR=32:1) | (CR=24:1) | (CR=16:1) | (CR=8:1) | (CR=4:1) | (CR=2:1) |

Fig. 19 Extracted watermark logo for JPEG 2000 quality scalability for full resolution scalability using non-blind extraction. *Row 1:* Without the model and *Row 2:* With the proposed model.
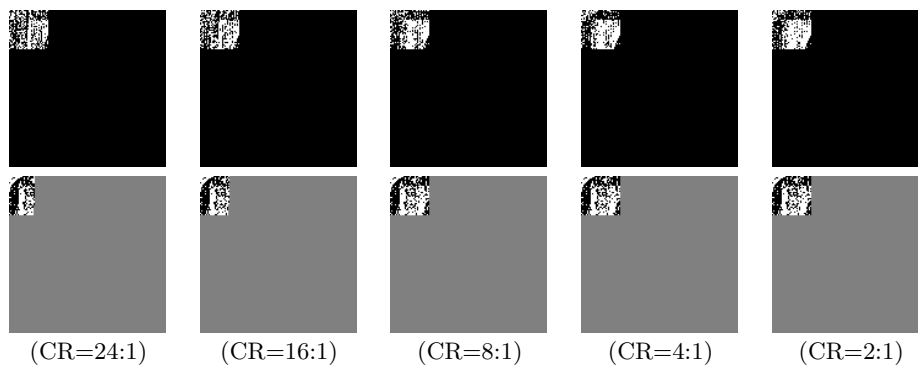
| (CR=24:1) | (CR=16:1) | (CR=8:1) | (CR=4:1) | (CR=2:1) |

Fig. 20 Extracted watermark logo for JPEG 2000 quality scalability for quarter resolution scalability using blind extraction. *Row 1:* Without the model and *Row 2:* With the proposed model.
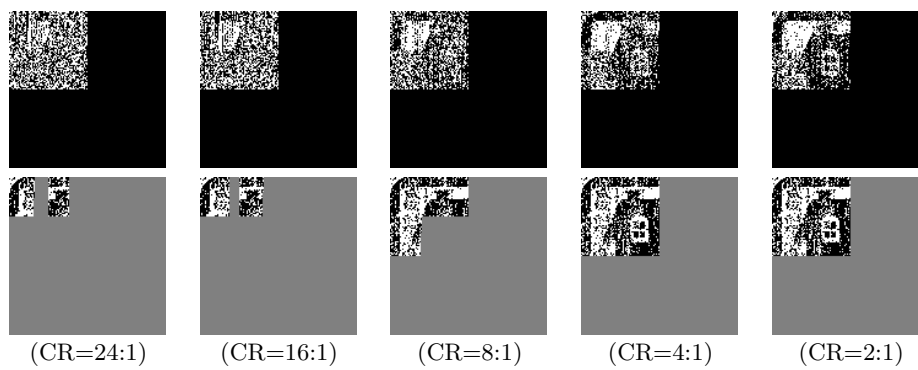

| (CR=24:1) | (CR=16:1) | (CR=8:1) | (CR=4:1) | (CR=2:1) |

Fig. 21 Extracted watermark logo for JPEG 2000 quality scalability for half resolution scalability using blind extraction. *Row 1:* Without the model and *Row 2:* With the proposed model.
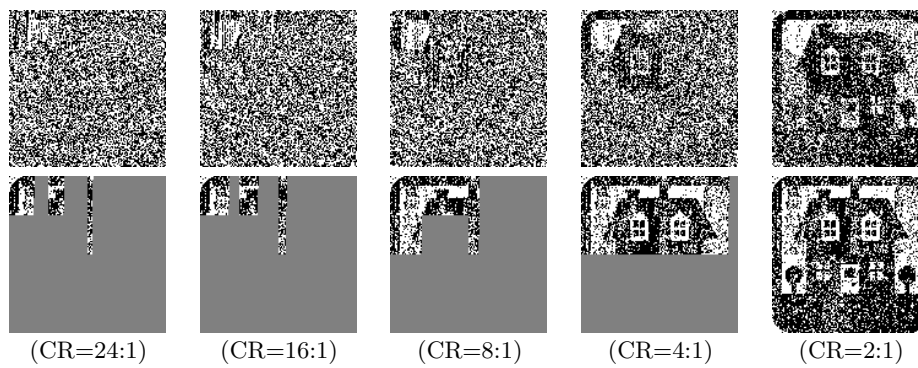

| (CR=24:1) | (CR=16:1) | (CR=8:1) | (CR=4:1) | (CR=2:1) |

Fig. 22 Extracted watermark logo for JPEG 2000 quality scalability for full resolution scalability using blind extraction. *Row 1:* Without the model and *Row 2:* With the proposed model.